Numerical flow simulations of a propeller design for an eVTOL vehicle using the Vortex Particle Method

3A internship report

presented by

Thomas Guignard

Company:
Deutsches Zentrum für Luft- und Raumfahrt – Antriebstechnik - Triebwerksakustik
Company supervisor:
Sébastien Guérin
SIGMA Clermont supervisor:
Yuri Lapusta

Date: March 2025 – August 2025

Référence du fichier : Guignard_ Thomas_RapportStage3A.pdf

SIGMA CLERMONT
CAMPUS DE CLERMONT-FERRAND – CS 20265 – 63178 AUBIERE– FRANCE
TEL. +33 (0)4 73 28 80 00 – FAX +33 (0)4 73 28 81 00 –https://www.sigma-clermont.fr/

FICHE D'IDENTIFICATION DU DOCUMENT

SIGMA+ 3A report

TITRE DU DOCUMENT :	Numerical flow simulations of a propeller design for an eVTOL vehicle using the Vortex Particle Method
AUTEUR(S) :	Thomas Guignard – Mechanical Engineering - MRS

Date du document	Nbre de pages	Référence du document
		Guignard_ Thomas_RapportStage3A.pdf

ABSTRACT:

This document presents an investigation of numerical flow simulations for a propeller design of an eVTOL vehicle using the Vortex Particle Method to predict aerodynamic interactions in different configurations.

Keywords: aircraft, aerodynamics, Vortex Particle Method, numerical simulation

RESUME :

Ce document présente une étude des simulations numériques de flux pour la conception d'une hélice d'un véhicule eVTOL utilisant la méthode des particules vortex afin de prédire les interactions aérodynamiques dans différentes configurations.

Mots clés : avion, aérodynamique, Vortex Particle Method, simulation numérique

Visa de l'entreprise :

Ce rapport de stage a été visé par (Nom, Prénom, Qualité) : Sébastien Guérin
Date : 20.08.2025
Signature :

Je demande que ce rapport soit confidentiel (non diffusé sur l'intranet de l'école) : ☐ OUI X NON

CONTENTS

Table of figures....6
Acknowledgments....7
1. Introduction....8
1.1. German Aerospace Center (DLR)....9
1.1.1. Institute of Technology Propulsion....9
1.1.2. Corporate culture and management....10
1.1.3. Sustainable Development....10
1.2. eVTOLUTION's project....10
2. Methodology....11
2.1. Vortex Particle Method....11
2.2. FLOWUnsteady Framework....12
2.2.1. Flow properties and solver characteristics....12
2.2.2. Rotor modelling approach within FLOWUnsteady....13
2.3. Aerodynamic modeling....15
2.3.1. Airfoil polars and lift-drag computation....15
2.3.2. Tip and loss correction....15
3. Application case: eVTOLUTION Rotor system....16
3.1. eVTOLUTION vehicle and rotor system overview....16
3.2. Rotor and wing geometry definition....17
3.2.1. Rotor geometry definition....17
3.2.2. Wing geometry definition....17
3.3. Operating conditions....18
4. Numerical simulations....19
4.1. Cruise....19
4.1.1. Cruise - 61 m/s case....19
4.1.2. Cruise - benchmark case....21
4.2. Hover....22
4.2.1. Front rotor....22
4.2.2. Aft rotor....26
4.3. Transition Climb and Transition Descent....27
4.3.1. Transition Climb....27
4.3.2. Transition descent....28

5. Observations 31
6. Conclusion and outlook 32
6.1. Conclusion 32
6.2. Outlook 33
7. Bibliography 34
Appendix A 35
Appendix B 36
Appendix C 37

Table of figures

Figure 1: Location of the different DLR offices in year 2025 [3] 9
Figure 2: Part of the JULIA script for the rotor generation 14
Figure 3: sectional view of propeller blade with forces 15
Figure 4: Distribution of the particles along the blade [4] 16
Figure 5: Vehicle planform and wingspan [3] 17
Figure 6: Geometry of the front (left) and aft (right) rotors within Paraview 17
Figure 7: Wing geometry definition 18
Figure 8: Reference mission profile [2] 18
Figure 9: Velocity Triangle Method 19
Figure 10: Comparison of the results of the front propeller isolated cruise (61 m/s) performance using different method 20
Figure 11: View of the simulation of the front benchmark case in the cruise configuration within Paraview at the last time step of the simulation 21
Figure 12: Comparison of the results of the front propeller isolated cruise benchmark performance using different method 21
Figure 13: Radial distribution of the thrust at the last time step of the simulation 22
Figure 14: Simulation showing numerical instabilities on the front rotor for the hover configuration (with box) 22
Figure 15: Evolution of the thrust over the time of the front hover rotor with basic setting without box 23
Figure 16: Prandtl tip loss model for two different corrections 24
Figure 17: Visualization of the particles after one rotation with (left) and without (right) the hub omission 24
Figure 18: Computational time for different setups tested for the front hover case 25
Figure 19: Evolution of the thrust over the time for different settings of the front hover rotor 25
Figure 20: Results of the front propeller isolated static performance of the experimental, BEMT and VPM methods 26
Figure 21: Results of the aft propeller static performance of the Experimental and VPM methods 27
Figure 22: Definition of the different velocities in the front of the propeller in the transition climb configuration 27
Figure 23: Longitudinal view of the aerodynamic behaviour in the transition climb configuration, illustrating the variation of the axial velocity within Paraview over one rotation; streamlines are shown 28
Figure 24: Definition of the different velocities in the front of the propeller in the transition descent configuration 29
Figure 25: Profile view of the aerodynamic behaviour in the transition descent configuration, illustrating the variation of the axial velocity within Paraview 30

Acknowledgments

First of all, I would like to express my sincere gratitude to my tutors, Sébastien Guérin and Tobias Lade, for their invaluable guidance and support throughout the duration of this internship. Their expertise, patience, and encouragement have been instrumental in the successful completion of this project. I deeply appreciate the time and effort they dedicated to mentoring me, and I am grateful for the insightful feedback and constructive criticism that helped shape my work.

I am also thankful to all the engineers of the team with whom I interacted for welcoming me and supporting me throughout the entire internship, and for answering my questions with good humour.

Finally, I am grateful to Yuri Lapusta, my SIGMA Clermont tutor, for supervising me.

1. Introduction

Acoustic studies play a crucial role in the evolution of modern aviation, especially in light of increasing environmental demands and the reduction of noise generated by aircraft. One of the major challenges for the aviation of the future is to make airplanes not only more environmentally friendly but also quieter. To achieve this goal, it is essential to assess noise generation from the design phase through to detailed component design. This approach involves the use of sophisticated models and tools to analyse and predict noise sources and their propagation.

The DLR Institute (Deutsches Zentrum für Luft- und Raumfahrt) of Propulsion Technology plays a key role in this pursuit of quieter aviation. Through its research, it focuses on reducing engine noise by studying noise excitation mechanisms and implementing noise reduction techniques at the source. The institute has several advanced tools and software at its disposal to carry out this work. Among these is PropNoise, a software developed in-house since 2008, which analyses the effects of noise generated by engines based on design parameters such as engine size, bypass ratio, and the number of blades. This analytical program is used to evaluate the acoustic characteristics of aircraft engines in the early design phase and is particularly valuable for early evaluations of future engines [1].

Other tools such as VIOLIN and CORAL complement this process by allowing the simulation of noise propagation and analysing its psychoacoustic impacts. VIOLIN simulates the propagation of noise to the ground during an aircraft flyover, while CORAL makes these sounds audible, providing a valuable tool for psychoacoustic studies. The Connect3D software, in turn, is used to prepare and analyse acoustic simulation results obtained through the CFD flow solver TRACE. This software includes advanced acoustic analysis methods and an interface with the PropNoise analysis tool, facilitating a detailed analysis of acoustic results in the context of engine design studies.

The goal of this report and the work carried out during this internship is to contribute to the advancement of noise studies in aviation by using the open-source software FLOWUnsteady. Building on the validation of the Vortex Particle Method (VPM) performed on the ENODISE B1 propeller model, the aim is to extend this approach to the eVTOLUTION project, which involves more complex rotor configurations. This continuity allows for the application of a validated numerical framework to new propulsion configurations, enabling a deeper analysis of aerodynamic interactions and their acoustic consequences. By studying these coupled phenomena in detail, the goal is to identify the mechanisms responsible for noise generation at the source and to support the development of effective mitigation strategies. Ultimately, these investigations aim to provide a transparent evaluation basis that enables policymakers and the public to understand both the minimum unavoidable and the technically achievable noise levels of eVTOL systems. This knowledge is essential for defining robust regulatory noise limits that protect communities from avoidable acoustic exposure.

1.1. German Aerospace Center (DLR)

DLR is the German aerospace research and technology centre and has been developing technologies for aeronautics and space, energy, transport, as well as security and defence research over 115 years.

Figure 1: Location of the different DLR offices in year 2025 [3]

DLR uses the expertise of its 54 research institutes and facilities to develop solutions to these challenges. Approximately 10,000 employees share a mission, to explore Earth and space and develop technologies for a sustainable future, where climate, mobility and technology are changing globally. By transferring technology, DLR contributes to strengthening Germany's position as a prime location for research and industry [1].

1.1.1. Institute of Technology Propulsion

The institute of Technology Propulsion is located in Cologne, Berlin, Göttingen and Trauen. Eight departments compose the institute: the combustion department, the combustor testing department, the fan and compressor department, the numerical method department, the engine department, the engine acoustics department, the engine measurement systems department, and the turbine department.

The Engine Acoustics Department, where the internship took place, focuses on the generation and propagation of noise in turbomachinery, as well as the design of future low-noise aircraft engines and gas turbines. Both numerical simulations and experimental investigations are employed to study the effects of unsteady flows, to localize moving noise sources using array measurement techniques,

and to reduce turbulence-related friction phenomena. In addition to conventional engine architectures, the department also investigates innovative propulsion concepts such as open rotors, which pose specific challenges in terms of noise generation and mitigation due to their complex aerodynamic interactions and strong tonal components.

1.1.2. Corporate culture and management

The German Aerospace Center employs approximately 10,000 people from almost 100 countries. DLR attaches great importance to the right framework conditions and a good and appreciate working environment. Employees in their diversity are given fair opportunities, modern career paths and flexible working models. Indeed, the staff is treated fairly, regardless of gender, nationality, ethnicity or social background, religion or ideology, disability age, sexual orientation and identity [1].

The institute of Technology Propulsion in Berlin is composed of different group of research where the management is different according to the group. However, different events are organized in order to share with the group and people like afterwork, lunch, or seminar where some researchers of the institute present their work. Moreover, weekly meetings were organized with the department to present results and discuss about issues and next goals.

1.1.3. Sustainable Development

DLR has committed itself to supporting national and international sustainable development goals through the expertise of its research fields: aeronautics, space, energy, transport, and cross-cutting research areas such as security, defence, and digitalization, as well as through the skills of project leaders at DLR and the German Space Agency within the DLR. In addition to research aimed at achieving and promoting sustainability goals, the DLR is also continuously developing the organizational structures and processes within the DLR to contribute as a publicly funded research organization [1].

1.2. eVTOLUTION's project

eVTOL (Electric Vertical Take-Off and Landing) vehicles represent a major technological development in the field of air transport. These electric vehicles are designed to take off and land vertically, allowing them to operate in urban environments without the need for large infrastructures like traditional runways. The use of electric motors reduces their carbon footprint and noise, making them particularly well-suited for densely populated urban areas. eVTOLs come in various designs, ranging from aircraft similar to helicopters to more innovative concepts, such as fixed-wing aircraft with distributed propulsion units across their wings. These vehicles are often envisioned for applications such as Urban Air Mobility (UAM), where they could revolutionize the way people travel in cities by reducing traffic congestion and offering a fast, environmentally friendly alternative to traditional transport. The challenges faced by eVTOLs include safety management, flight range, charging infrastructure, and the adaptation of air regulations to these new technologies. However, with ongoing advancements in battery technology and electric propulsion systems, eVTOLs are well on their way to becoming a viable solution for future mobility.

The eVTOLUTION project (Electric Vertical Take-Off and Landing Aircraft Optimization through Low-fidelity Unsteady Tools and Intelligent mOdelliNg) is a research program funded by the European Union under the Horizon Europe framework. It started in 2025 and brings together a consortium of universities, research institutes, and industrial partners from across Europe. The main objective of the project is to develop a numerical simulation framework for the design and optimization of electric vertical take-off and landing (eVTOL) aircraft. The methodology combines low-, medium-, and high-fidelity simulation tools, along with surrogate modelling techniques based on artificial intelligence, with the aim of reducing computation times and accelerating design space exploration. The project addresses topics such as unsteady aerodynamic modelling, aeroacoustics, thermal management, and flight stability, with a focus on the early-stage design of eVTOL configurations suitable for urban environments. It also involves cross-validation between numerical predictions and experimental data. The project consortium includes the following partners as different universities: TU Delft, University of Bristol, Politecnico di Torino, Vrije Universiteit Brussel, Università degli Studi Roma Tre; research institute: German Aerospace Center (DLR), Von Kármán Institute for Fluid Dynamics; and industrial partners: GKN Aerospace, Vertical Aerospace, Mejzlik Propellers, Heathrow Airport [6].

2. Methodology

2.1. Vortex Particle Method

The Vortex Particle Method (VPM) is a mesh-free technique used in computational fluid dynamics to solve the Navier-Stokes equations in their velocity-vorticity form. This method employs a Lagrangian framework, which eliminates the challenges associated with mesh generation. It also preserves vortical structures over long distances with minimal numerical dissipation, offering significant speed advantages over traditional mesh-based CFD approaches. However, VPM is known to become numerically unstable when vortical structures deteriorate near the turbulent regime. The reformulated VPM uses a Lagrangian scheme to solve the vorticity form of the LES-filtered Navier-Stokes equations [4]:

$$\frac{\partial \overline{\omega_\iota}}{\partial t} + \overline{u_J}\frac{\partial \overline{\omega_\iota}}{\partial x_j} = \overline{\omega_J}\frac{\partial \overline{u_\iota}}{\partial x_j} + \nu\nabla^2\overline{\omega_\iota} - \frac{\partial T'_{ij}}{\partial x_j} + \frac{\partial T_{ij}}{\partial x_j} \quad \textbf{(1)}$$

The bar indicates the filter operator, and $T_{ij} = \overline{u_\iota w_J} - \overline{u_\iota}\,\overline{w_J}$ represents the subfilter-scale vorticity stress, which captures the interactions between large-scale and subfilter-scale (SFS) dynamics. The term $\frac{\partial T'_{ij}}{\partial x_j}$ accounts for the SFS contributions from the advective term (vorticity advection), while $\frac{\partial T_{ij}}{\partial x_j}$ represents the contributions from stretching. For simplicity, equation (1) is expressed in vector form as:

$$\frac{d}{dt}\overline{\omega} = (\overline{\omega}.\nabla)\overline{u} + \nu\nabla^2\overline{\omega} - E_{adv} - E_{str} \quad \textbf{(2)}$$

Where $(E_{adv})_i = \frac{\partial T'_{ij}}{\partial x_j}$ represents the SFS vorticity advection, $(E_{str})_i = \frac{\partial T_{ij}}{\partial x_j}$ denotes the SFS vortex stretching, and the $\frac{d}{dt}$ operator is the linearized form of the filtered material derivative, $\frac{d}{dt}() = \frac{\partial}{\partial t}() +$

$(\bar{u}.\nabla)()$. It is important to note that expressing the Navier-Stokes equations in vorticity form removes the dependence on pressure. Moreover, this formulation depends on the vorticity field $\omega = \nabla$ x u through the Biot-Savart law.

This mesh-free LES method relies on the assumption of incompressible flow, which is valid for low Mach number applications typical of eVTOL propulsion. The reformulated Vortex Particle Method (rVPM) presents several advantages over traditional mesh-based CFD approaches. By avoiding mesh generation altogether, rVPM eliminates the time-consuming process of creating a high-quality mesh and prevents errors associated with poor mesh resolution. While coarse discretization is also possible with mesh-based methods, rVPM achieves comparable physical accuracy without numerical dissipation introduced by grid interpolation. Derivatives are computed analytically rather than using stencil-based approximations. Additionally, the method is computationally efficient, as it concentrates computational effort only in regions containing vorticity, unlike mesh-based methods that discretize the entire domain, leading to performance gains of up to two orders of magnitude compared to conventional mesh-based LES, without compromising accuracy.

2.2. FLOWUnsteady Framework

FLOWUnsteady is a numerical simulation software primarily used for analysing unsteady aerodynamic flows, with a particular focus on rotorcraft and eVTOL applications [3]. It is based on the Vortex Particle Method (VPM), a mesh-free approach that solves the vorticity formulation of the incompressible Navier–Stokes equations as explained in the previous section. This method is well suited for capturing unsteady flow phenomena such as wake development, vortex shedding, and rotor, wake interactions. FLOWUnsteady has been developed by Eduardo J.Alvarez, a doctoral student at Brigham Young University, in collaboration with Judd Mehr and Andrew Ning. It was first introduced at the AIAA aviation Forum in June 2022.

FLOWUnsteady does not rely on traditional turbulence models like the k–ε RANS model; instead, its treatment of turbulence is intrinsically similar to a Large Eddy Simulation (LES), where large-scale vortical structures are resolved directly, and sub-filter scale effects are modelled. This allows for detailed investigation of lift, drag, and stability characteristics under time-varying flow conditions.

The software supports simulations of both vertical flight (hover) and forward flight, enabling the analysis of rotor and lifting surface performance in realistic mission phases. Additionally, FLOWUnsteady includes tools for evaluating and optimizing aerodynamic configurations with respect to performance and noise generation, key concerns for the integration of eVTOL vehicles in urban environments [3].

2.2.1. Flow properties and solver characteristics

The flow properties used in FLOWUnsteady were defined based on the ideal gas assumption, for the standard atmospheric conditions. The static values prescribed were the static pressure $P_s = 101325\ Pa$ and static temperature $T_s = 298.15\ K$. The specific gas constant for air was taken as $R = 287.06\ Jkg^{-1}K^{-1}$, and the heat capacity ratio was γ=1.4.

The static density was computed using the ideal gas law:

$$\rho_s = \frac{P_s}{RT_s} = 1{,}1834\ kg/m^3 \qquad \textbf{(5)}$$

The speed of sound, which depends on the static temperature, was given by:

$$c = \sqrt{\gamma RT} = 346.152\ m/s \qquad \textbf{(6)}$$

These values were used to compute the Mach number M for each flight condition. The total (or stagnation) pressure and temperature, assuming isentropic flow, were obtained from the following relations:

$$P_t = P_s(1 + \tfrac{\gamma-1}{2}M^2)^{\frac{\gamma}{\gamma-1}} \text{ and } T_t = T_s(1 + \tfrac{\gamma-1}{2}M^2) \qquad \textbf{(7)}$$

These parameters were then used to define the fluid inlet conditions in the simulations with the in-house CFD solver TRACE, depending on the prescribed flow velocity for each rotor configuration.

2.2.2. Rotor modelling approach within FLOWUnsteady

In FLOWUnsteady, rotors are defined using a built-in function that constructs the blade geometry by stacking two-dimensional airfoil profiles along the blade span. This can be done either by providing a set of geometric distributions, such as twist, chord, and sweep, or by reading these distributions from an external file. This is the only way rotor geometry can be described within FLOWUnsteady.
The key parameters used to define the rotor geometry are:

- Chord: distance between the blade leading and trailing edges.
- Twist: the variation of the local stagger angle of attack (relative to the rotor axis) along the span, used to adapt blade loading to local flow conditions.
- Sweep: the lateral displacement or inclination of the blade sections along the span.
- Height offset: the vertical displacement of blade sections, used to model dihedral or geometric elevation effects.

Each blade section is associated with a 2D airfoil, which defines its aerodynamic characteristics. The performance of each airfoil is described by polars, i.e., curves showing the relationship between the angle of attack (α) and the corresponding lift (Cl) and drag (Cd) coefficients. These polars are essential for predicting local aerodynamic forces and overall rotor performance. For example, at low angles of attack, lift and drag remain low; as the angle increases, lift grows until a critical point is reached where the flow separates, leading to stall and a sharp drop in lift [7].
By stacking 2D profiles with specified geometric distributions, FLOWUnsteady generates a full 3D representation of the rotor suitable for unsteady aerodynamic simulations.

The rotors were generated by a Julia script where rotor parameters, discretization settings, airfoil processing and output options are defined, as defined in figure 2.

```
generate_rotor(Rtip, Rhub, B,
                    chorddist, twistdist, sweepdist, heightdist,
                    airfoil_contours;

                    # MORE ROTOR PARAMETERS
                    pitch=0.0,
                    CW=true,

                    # DISCRETIZATION SETTINGS
                    n=10, blade_r=1.0,
                    rediscretize_airfoils=true,
                    rfl_n_lower=15, rfl_n_upper=15,
                    spline_k=5, spline_s=0.001, spline_bc="extrapolate",

                    # AIRFOIL PROCESSING
                    data_path=FLOWUnsteady.default_database,
                    read_polar=vlm.ap.read_polar,
                    xfoil=false,
                    alphas=[i for i in -20:1.0:20], ncrit=9,
                    ReD=5e5, altReD=nothing, Matip=0.0,

                    # OUTPUT OPTIONS
                    verbose=false, verbose_xfoil=false, v_lvl=1,
                    plot_disc=true, save_polars=nothing)
```

Figure 2: Part of the JULIA script for the rotor generation

This script defines various parameters for simulating rotor performance and airfoil processing.

- **pitch (Real, deg)**: Rotor collective pitch angle.
- **CW (Bool)**: Direction of rotor rotation, true for clockwise, false for counter-clockwise.
- **Discretization**:
  - **n (Int)**: Number of blade elements per blade.
  - **r (Real)**: Ratio of spacing between elements at the tip to that at the root.
  - **spline_k (Int), spline_s (Real), spline_bc (String)**: Parameters for spline-based blade discretization using the Dierckx package. spline_k is the spline order, spline_s is the smoothing parameter, and spline_bc specifies boundary conditions.
  - **rediscretize_airfoils (Bool)**: If true, it rediscretizes airfoil contours using panels, with separate discretization for the upper and lower contours.
- **Airfoil Processing**:
  - **data_path (String)**: Path to the airfoil polar database.
  - **read_polar (Function)**: Function for parsing airfoil files (vlm.ap.read_polar for XFOIL outputs, vlm.ap.read_polar2 for CSV).
  - **xfoil (Bool)**: If true, overrides polar files and generates new polars using XFOIL, with sweep angle of attack (AOA) and turbulence parameter.
  - **ReD (Real), Matip (Real), altReD (Tuple)**: Reynolds number based on diameter, rotational and freestream Mach numbers. These are used in XFOIL calculations for airfoil polars or can be ignored if polars are pre-supplied.
  - **altReD (Tuple)**: Calculates Reynolds number based on effective velocity for each station, which is more accurate but not required.
  - **Note**: Deactivate compressibility corrections in XFOIL when Matip ≠ 0 to avoid double-counting compressibility effects.

This set of parameters facilitated detailed rotor simulation and airfoil analysis, including discretization, airfoil processing via XFOIL, and output generation for verification and debugging.

2.3. Aerodynamic modeling

2.3.1. Airfoil polars and lift-drag computation

During the aerodynamic study, four main aspects were investigated: the airfoil boundary layer, the airfoil forces, the rotor forces, and rotor tip losses. The performance of the propeller was analyzed using the XFOIL software. The aerodynamic model of a propeller blade is illustrated in Figure 3. The forces acting on the blade include the sectional lift ΔL, drag ΔD, thrust ΔT, and torque ΔQ, where the delta symbol indicates that these quantities correspond to an elemental blade section of depth Δr. These sectional forces were subsequently integrated along the blade span to determine overall rotor performance. They were also used in the model validation and in the aerodynamic study of the propeller system [5].

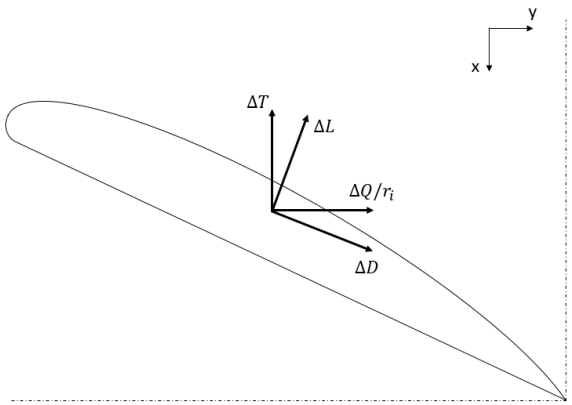

Figure 3: sectional view of propeller blade with forces

2.3.2. Tip and loss correction

In order to model the interaction between the blade and the surrounding fluid, the aerodynamic forces acting along the blade were reintroduced into the flow domain in the form of immersed vorticity. This conversion was based on the Kutta–Joukowski theorem, which expresses aerodynamic lift as a circulation distribution:

$$\Gamma = \frac{1}{2} c \,.\, V_{local} C_l \quad \textbf{(3)}$$

where ccc is the local chord length of the blade element and V_{local}, is the relative velocity experienced by that element. This circulation was represented by vortex particles placed along the blade surface to model the spanwise lift distribution (see Figure 4). At the trailing edge, these bound particles shed free vortex particles into the wake, capturing unsteady effects such as fluctuations in aerodynamic loading and trailing-edge circulation. In addition to lift, the blade also experiences viscous drag, which could be modeled by introducing force dipoles of strength $\mu = V_{local} \,.\, C_d$, , aligned along the flow direction, forming so-called dragging lines. However, in the configurations studied here, this viscous contribution had a comparatively minor effect on the overall flow field and forces, referred to as a second-order effect, and was therefore neglected for computational efficiency. The frequency of particle shedding per rotor revolution defines the initial spacing Δ_x between vortex particles, while the core size σ determines the spatial resolution of the wake. The accuracy of the blade representation also depended on the number of discrete elements used along the blade span, see figure 4.

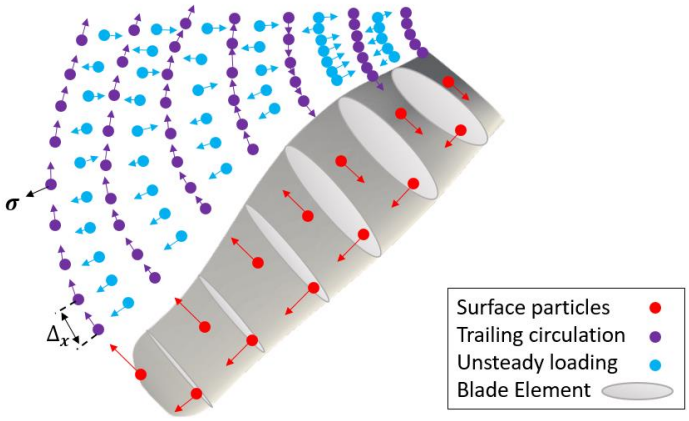

Figure 4: Distribution of the particles along the blade [4]

To improve the aerodynamic modeling accuracy of the rotor, a hub and tip loss correction was applied in the Vortex Lattice Method (VLM) solver via the `hubtiploss_correction` parameter. This correction accounts for the reduction in lift observed near the blade root (hub loss) and blade tip (tip loss), which is caused by the formation of tip vortices and the hub geometry. The correction used is based on an empirical, Prandtl-like model, applied to the affected blade panels:

$$F_{tip} = \frac{2}{\pi} cos^{-1}(\exp(-f_{tip})) \text{ , where } f_{tip} = \frac{B}{2} \frac{[(\frac{R_{rotor}}{r})^{t_1} - 1]^{t_2}}{|\sin(\theta_{eff}|^{t_3}} \quad \textbf{(4)}$$

$$F_{hub} = \frac{2}{\pi} cos^{-1}(\exp(-f_{hub})) \text{ , where } f_{tip} = \frac{B}{2} \frac{[(\frac{r}{R_{hub}})^{h_1} - 1]^{h_2}}{|\sin(\theta_{eff}|^{h_3}} \quad \textbf{(5)}$$

Where R_{rotor} and R_{hub} are the radius rotor tip and hub, B is the number of the blades, r is the radial position of the blade element, and t_1, t_2, t_3, h_1, h_2, and h_3 are tunable parameters.
This method improved the representation of the actual lift distribution along the blade span and enhanced the accuracy of rotor performance predictions [4].

3. Application case: eVTOLUTION Rotor system

3.1. eVTOLUTION vehicle and rotor system overview

In the eVTOLUTION project, the aircraft featured a wingspan of 15 meters and a maximum take-off weight of 3150 kg and a normal cruising speed of 120 knots (220 km/h), see figure 5. It is equipped with a total of eight propellers: four tilting propellers mounted forward of the wing and four lift-only propellers positioned aft of the wing. The front and rear propellers are characterized by distinct geometric designs, tailored to their specific aerodynamic roles.

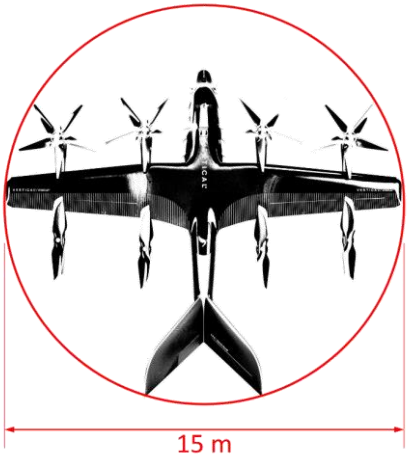

Figure 5: Vehicle planform and wingspan [3]

3.2. Rotor and wing geometry definition

3.2.1. Rotor geometry definition

The location of each propeller was defined relative to the wing's 25%-chord line, and the reference hub point was taken as the intersection of the blades' 25%-chord lines. This standardized positioning enabled consistent modeling of aerodynamic forces and moments. To enhance safety during vertical flight, all propellers were tilted by 5 degrees around the aircraft's longitudinal (x-) axis in hover. This tilt helps prevent potential cascade failure and a phenomenon in which wake interference between propellers can lead to stall and a rapid, uncontrollable loss of lift across multiple rotors. The geometries of the front and aft rotors are different: the front propeller consists of five blades with a variable pitch and a specific blade design, while the aft rotor has four blades with a fixed pitch and its own distinct geometry (see Figure 6). These design differences were implemented to meet the specific aerodynamic requirements of each rotor.

Figure 6: Geometry of the front (left) and aft (right) rotors within Paraview

3.2.2. Wing geometry definition

The airfoil used for the outboard pylon is a NACA 2416 profile, while the airfoil used for the inboard pylon is a NACA 4418 profile, see figure 7.

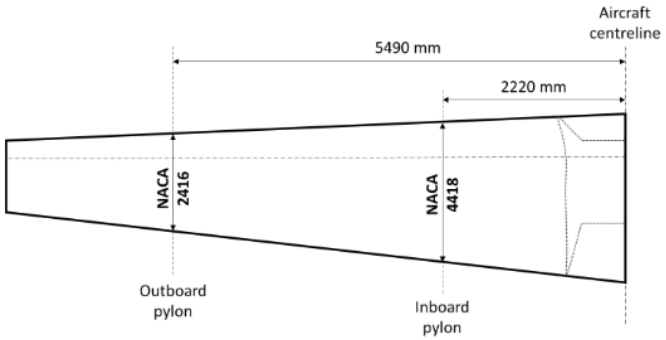

Figure 7: Wing geometry definition

3.3. Operating conditions

In this study, five rotor system configurations, namely A1, A2, A4, B1, and B2, are examined under five distinct flight conditions, as detailed in Appendix A [2]. These operating points represent key phases of a typical eVTOL mission profile: hover, transition climb, cruise, transition descent, and an emergency condition (see Figure 8). Each flight condition corresponds to a specific aerodynamic environment and rotor loading scenario. The hover phase simulates vertical take-off or landing, where lift is generated solely through rotor thrust while the aircraft remains stationary or nearly stationary. The transition climb represents the forward acceleration after take-off, requiring both vertical lift and forward propulsion. The cruise condition corresponds to steady, horizontal flight at constant speed and altitude, typically the most aerodynamically efficient regime. The transition descent mirrors the climb phase in reverse, with the vehicle decelerating and preparing for vertical descent. Finally, the emergency condition simulates a critical scenario in which one propulsion unit must generate double thrust to compensate for the failure of a second unit (either motor or propeller), representing a demanding and safety-critical load case.

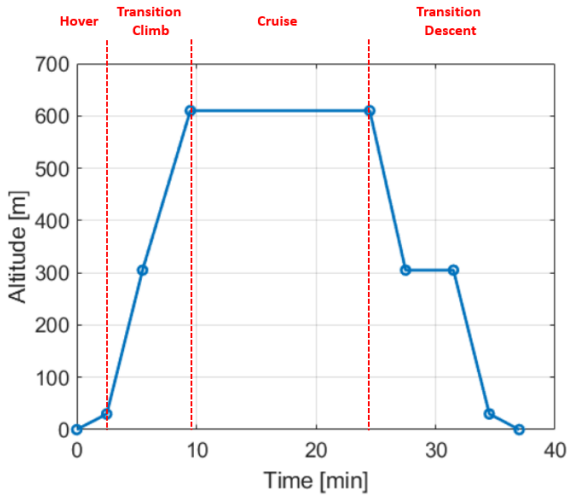

Figure 8: Reference mission profile [2]

4. Numerical simulations

Numerical simulations and model validation using new methods present a complex challenge in engineering and research. Achieving an accurate and reliable model requires meticulous parameter adjustment, often involving multiple simulation runs to refine these settings. This iterative process is crucial to ensure the model closely reflects real-world conditions. Once a satisfactory model is established, it serves as a benchmark for subsequent simulations, enabling deeper analysis and optimization of the systems under study. Indeed, in order to verify the correct operation of the model it is necessary to generate different simulations and check several things:

- If this file runs correctly with the solver until the end of the defined calculation time
- and that the result file seems to provide physically results with a satisfactory accuracy

This chapter is based on five flight configurations, each corresponding to a specific operating point, as presented in Appendix B. The numerical study is structured into two main parts. The first focuses on the hover and cruise cases, aiming to validate a reference simulation setup and assess the performance of the Vortex Particle Method (VPM) applied to eVTOLUTION geometries. The second part addresses the transition climb and descent cases, with the objective of analysing aerodynamic interactions between rotors that certainly contribute to strongly increase the noise generation.

4.1. Cruise

In the cruise configuration the front rotor was tilted at 0 degrees, (that is, the rotor axis in parallel to the aircraft fuselage), while the rear rotors are tilted at 90 degrees in a fan-folded configuration with two overlapping blades. Simulations were performed under this setup with the objective of establishing a reference configuration for the front rotor.

4.1.1. Cruise - 61 m/s case

In the cruise case, a preliminary study was conducted to determine the appropriate blade pitch angle, as this value had not been specified before. Indeed, the data table only provided the target thrust value and the indication *"hover +14°"*. Based on this information, and using the velocity triangle method in figure 9, an approximate pitch angle was estimated.

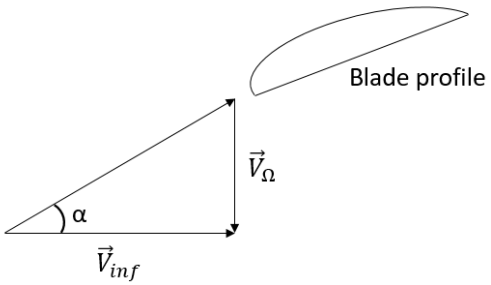

Figure 9: Velocity Triangle Method

Where:

$$V_\Omega = \Omega \,.\, r = 2\pi \,.\, rps \,.\, 0{,}75R \quad \textbf{(6)}$$

$$V_{inf} = 30\ m/s\ or\ 61\ m/s$$

In this study, two operating points were investigated: one with an inflow velocity V_{inf} of 61 m/s, and the other one with V_{inf} of 30 m/s (benchmark case), both using an initial blade pitch angle of 14°. To determine the pitch angle in the cruise configuration, the difference $\alpha_{30} - \alpha_{61}°$ was added to the initial pitch.

$$\alpha_{30} = \arctan\left(\frac{V_\Omega}{V_{inf}}\right) = \arctan\left(\frac{2\pi . \frac{5000}{60} .0{,}75 .0{,}1515}{30}\right) = 63{,}5° \quad \textbf{(7)}$$

$$\alpha_{61} = \arctan\left(\frac{V_\Omega}{V_{inf}}\right) = \arctan\left(\frac{2\pi . \frac{5000}{60} .0{,}75 .0{,}1515}{61}\right) = 44{,}4° \quad \textbf{(8)}$$

With the equations (7) and (8), $\alpha_{30} - \alpha_{61} = 19{,}1°$ and the cruise pitch 14° + 19,1° = 33,1°.
Using this approximate value, an initial simulation was run to verify the resulting thrust and to establish a thrust vs. pitch angle trend. This trend was then refined through additional simulations.

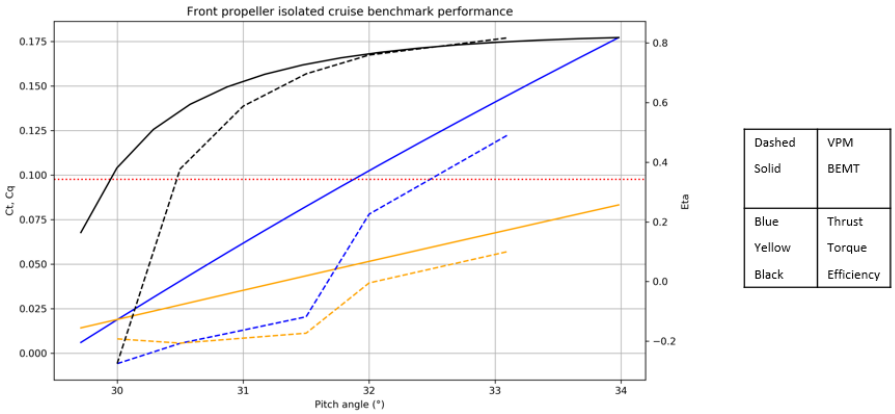

Figure 10: Comparison of the results of the front propeller isolated cruise (61 m/s) performance using different method

Figure 10 shows the variation of thrust with respect to the blade pitch angle. In this figure, both BEMT and VPM simulations follow a similar trend, indicating a good qualitative agreement between the two models. However, the VPM curve should be more straight as the BEMT curve. For a target thrust of 6.5 N (this targeted value is indicated by the red dotted line), both approaches predicted pitch angles of the same order of magnitude, which reinforced the consistency of the results. This plot highlights the great sensitivity of pitch angle on the aerodynamic behavior of the rotor. Indeed, small variations in pitch can lead to significant changes in thrust, especially at high axial velocities (such as 61 m/s in this case). Under these conditions, a slight decrease in pitch may even result in negative thrust, meaning the rotor starts operating in a braking mode, acting against the incoming flow. This phenomenon is particularly important in the context of the studied eVTOL configuration, as it demonstrates the sensitivity of rotor performance to incidence angle at high-speed flight conditions. It underlines the necessity of properly adapting the blade pitch to ensure optimal performance and to avoid undesirable operating regimes.

4.1.2. Cruise - benchmark case

In the benchmark case, the axial inflow velocity was set to 30 m/s, a value specifically chosen to ensure compatibility with wind tunnel testing, where the maximum achievable freestream velocity is limited to this value. The blades of the front rotor were assigned a pitch angle of 14°. During the initial simulations using the basic setup, the results already demonstrated stable behavior and good convergence, as shown in Figure 11. This robustness enabled a direct transition to the high-fidelity setup and allowed for meaningful comparisons with reference data such as BEMT predictions, RANS simulations, and experimental measurements.

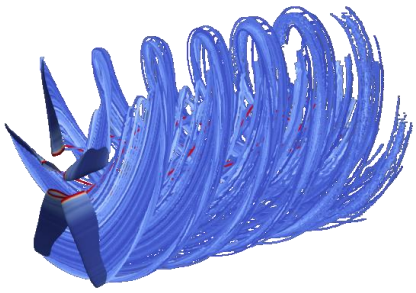

Figure 11: View of the simulation of the front benchmark case in the cruise configuration within Paraview at the last time step of the simulation

Indeed, Figure 12 presents the results from RANS (steady aerodynamics), VPM (non-steady Lagrangian method), and BEMT (analytical approach), using the same XFOIL polars.

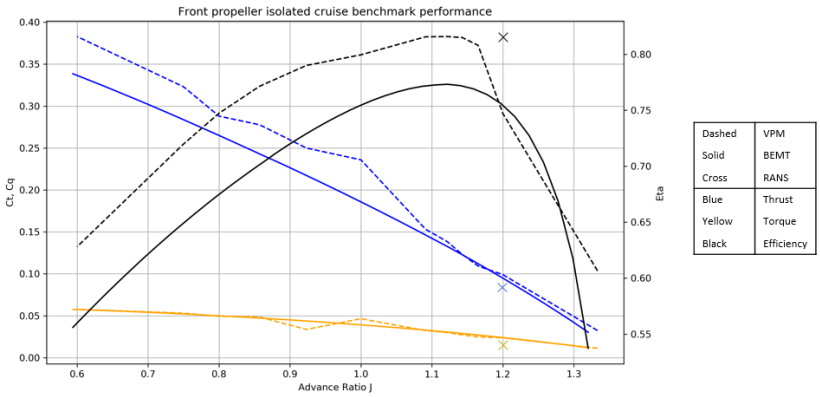

Figure 12: Comparison of the results of the front propeller isolated cruise benchmark performance using different method

Although the overall trend of the curves from the different methods is similar, significant differences in the computed values are observed across the operating points. This discrepancy is particularly surprising between the VPM and BEMT methods, since both simulations use the same polars data from XFOIL. Moreover, the RANS results appear to deviate significantly from the others, as shown in Figure 13, where the radial distribution of thrust and torque is compared for the different approaches. In this figure, the RANS results exhibit a clear offset. That said, the slight discrepancy between VPM and BEMT had already been observed during the validation of the VPM method using the ENODISE model. A similar behavior is found in the current model, which remains unexplained and is still under investigation, especially in the hover configuration. One possible explanation lies in the absence of a spinner-hub in the FLOWUnsteady and BEMT setups. In FLOWUnsteady, only lifting lines can be used, as for the wing, to model e.g the rotor–wing interactions. Remark the poor performance

with a negative thrust near the hub location all the simulation results, including the RANS with spinner—hub, see Figure 13.

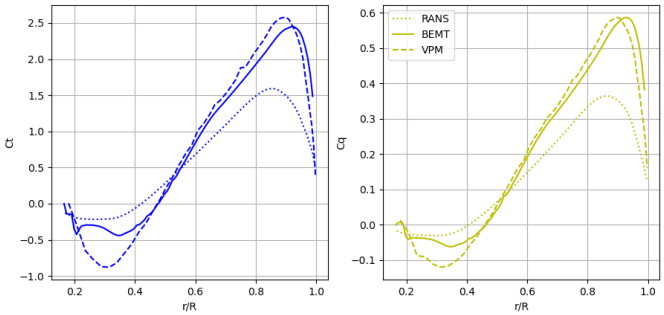

Figure 13: Radial distribution of the thrust at the last time step of the simulation

4.2. Hover

In the hover configuration, the aircraft is static and therefore subjected to zero initial velocity. Both the front and rear rotors are tilted at 90 degrees. Simulations were carried out under this configuration with the objective of establishing a reference setup for each rotor.

4.2.1. Front rotor

The front rotor, with five blades in the horizontal position and the reference pitch, operated at 8300 RPM in a hover condition without axial inflow. Simulations were run using FLOWUnsteady's initial mid-fidelity setup as a good compromise between accuracy and computational cost. In the first simulations, a particle box was placed downstream to limit the tracking to a smaller physical domain, reducing memory and disk usage. Under these conditions $V_{inf} = 0\, m/s$, the wake showed non-physical behavior: without axial convection, vortex particles stagnated or recirculated near the rotor, disrupting wake structure and stability. This led to particle accumulation downstream and near the hub, sometimes causing sudden upstream ejections resembling artificial "explosions" due to numerical instabilities, see figure 14. These results underline the sensitivity of hover simulations to axial flow conditions and the need for careful downstream domain treatment to avoid numerical instabilities.

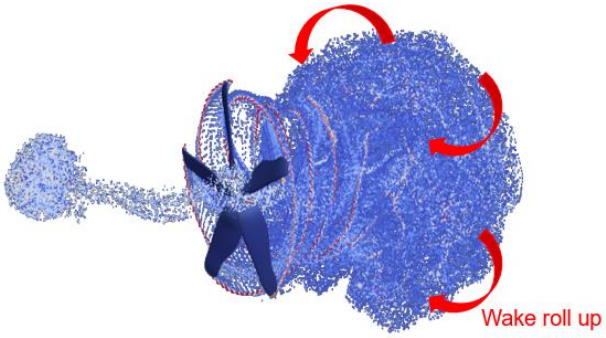

Figure 14: Simulation showing numerical instabilities on the front rotor for the hover configuration (with box)

This downstream accumulation of particles introduced a strong unsteadiness in the rotor thrust. As the vortex particles gathered in the wake region, the local induced velocities around the rotor blades were progressively altered, leading to an artificial increase in thrust. Once a critical concentration of particles was reached, the rotor abruptly expelled the excess vorticity, causing a

sudden drop in thrust, see figure 15 without the use of a downstream box. This cycle repeated periodically, resulting in oscillatory behavior in the thrust signal that did not correspond to any physical phenomenon. These thrust fluctuations, directly linked to the unphysical massing of particles in the near wake, significantly reduced the reliability of the simulation under these flow conditions.

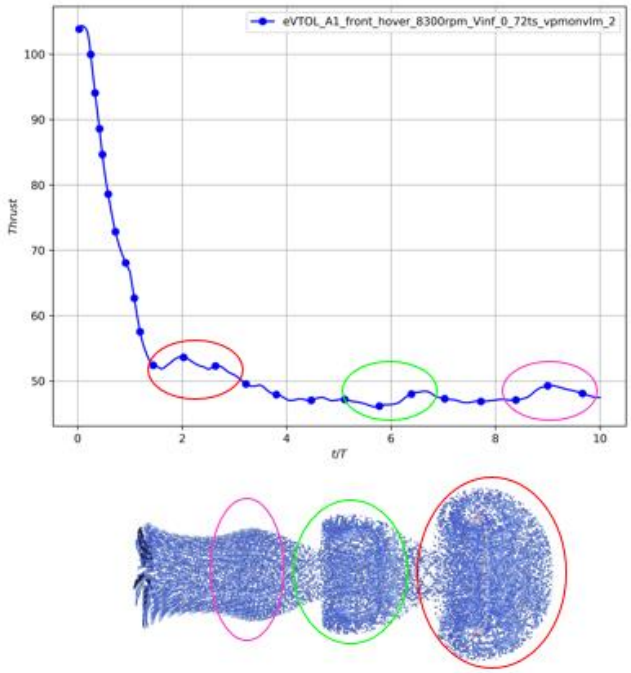

Figure 15: Evolution of the thrust over the time of the front hover rotor with basic setting without box

To mitigate these effects, a particle box was implemented. Its purpose was twofold: to prevent the unphysical accumulation of vortex particles in the near wake region, while ensuring that a sufficient number of particles were captured to preserve a realistic physical behavior of the flow. By constraining particle generation and retention within a defined spatial domain, the simulation maintained better stability while still allowing the key aerodynamic interactions to be resolved. The particle box clearly limits the vortex particles to a predefined spatial domain. Any particles moving beyond this region were no longer considered in the simulation, which helped control numerical instabilities without compromising the physical relevance of the near-field wake.

Moreover, during the validation process of the propeller model, the application of Prandtl's tip and hub loss model, as expected, produced some discrepancies in the predicted aerodynamic performance near the hub region, as shown in Figure 16. We conducted that the modified hub loss function demonstrated better convergence and a more realistic representation of the flow effects close to the hub. This modified function imposes a higher penalty on the forces generated by airfoils near the hub, resulting in the generation of particles with reduced vorticity in these regions. Consequently,

the aerodynamic loading is more accurately captured, particularly in the hub area where classical Prandtl loss models tend to overestimate performance

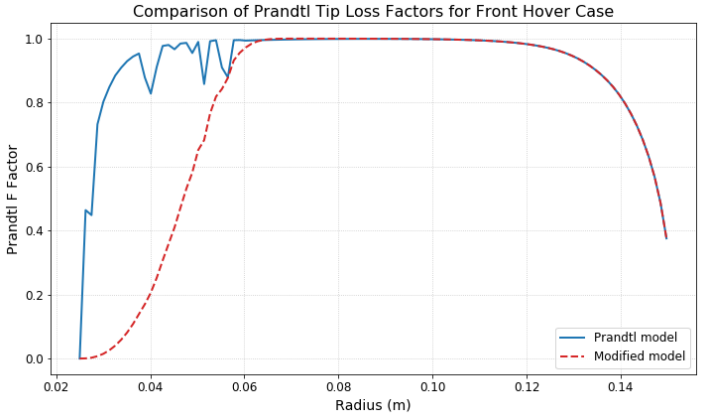

Figure 16: Prandtl tip loss model for two different corrections

This indicated that the simulation struggled to properly capture the unsteady vortex dynamics and flow structures in this area, which is typically characterized by complex interactions and limited circulation. To address this, several strategies were explored to improve both the stability and convergence of the VPM (Vortex Particle Method) simulations.

First, a filtering technique was implemented that temporarily deactivated the contribution of particles near the hub over an initial portion of the simulation. Specifically, particles within 30% of the blade span from the hub were disregarded during the first 3 revolutions, see figure 17.

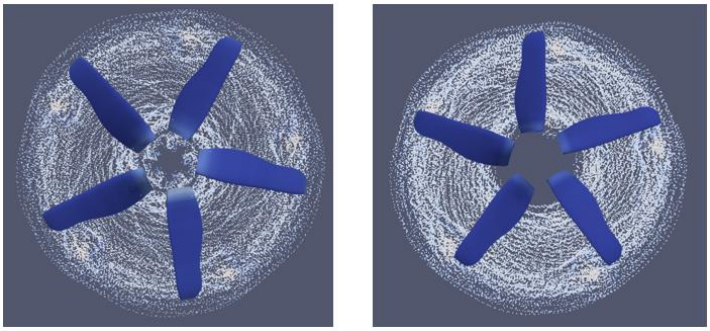

Figure 17: Visualization of the particles after one rotation with (left) and without (right) the hub omission

This was done to allow the wake development to stabilize without interference from potentially unstable near-hub contributions in the early transient phase. Since this approach does not affect the weak formation but rather targets the near-hub region specifically, it is more appropriate to refer to it as a near-hub particle exclusion method rather than a "wake treatment." Next, simulations were conducted using the Subfilter-Scale (SFS) model, which introduces additional viscous-like dissipation to improve numerical robustness and physical accuracy. While the use of SFS clearly helped dampen instabilities and led to smoother convergence behavior, it significantly increased the computational cost, making it less suitable for large parameter sweeps or long-time simulations, see figure 18.

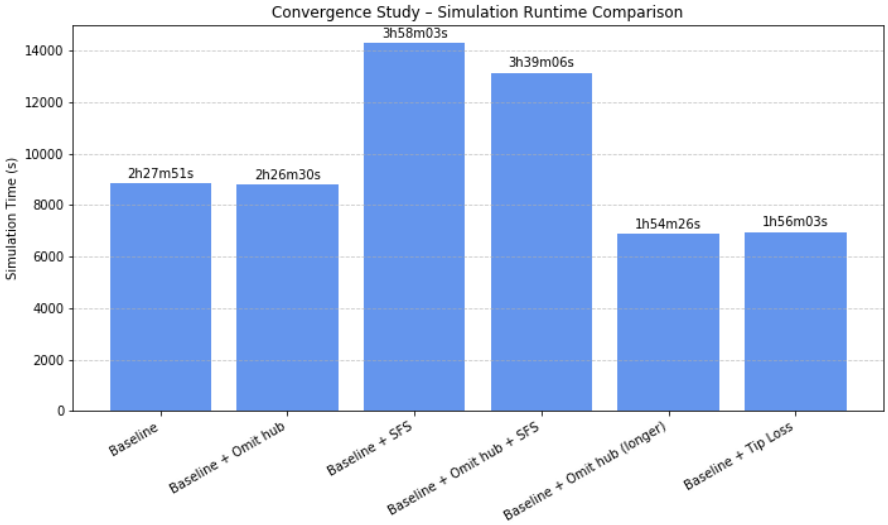

Figure 18: Computational time for different setups tested for the front hover case

Subsequently, a combination of both techniques, near-hub particle exclusion and the SFS model, was tested to assess whether the benefits of each method could be synergized. While this approach provided the most stable results, the added cost of the SFS model remained a concern.
Finally, an alternative hub-tip loss correction was applied in the VLM formulation to verify its influence on performance prediction. In the end, the near-hub particle exclusion method alone was found to offer the best trade-off: it reduced early-time numerical oscillations and improved convergence while maintaining reasonable computational efficiency. As such, it was selected as the preferred strategy for further simulations.

The following results in figure 19 present the time evolution of the thrust force computed over the entire rotor. This global thrust was obtained by integrating the local aerodynamic forces on all blades over the full rotor disk. It provided a direct indication of the rotor's global performance under the specified flow conditions. The plots highlight how the thrust varies over time and allow for comparisons between different rotor configurations or numerical treatments (e.g., with or without hub omission).

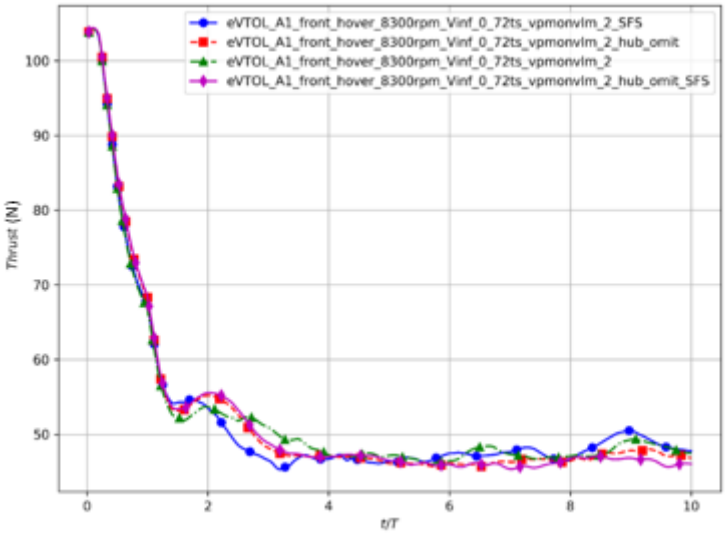

Figure 19: Evolution of the thrust over the time for different settings of the front hover rotor

In fact, several additional investigations were carried out on the hover case, but none of them produced better results than those presented in this report. Various simulation strategies were tested, such as imposing a minimum freestream velocity V_{inf} of 2 m/s to reduce wake accumulation downstream of the rotor, adjusting blade discretization parameters, or introducing viscous effects to improve the flow behavior. However, these changes did not lead to any improvement in the simulation accuracy and, in some cases, significantly increased computation time.

Yet, the objective of the VPM method and the FLOWUnsteady solver is precisely to simulate unsteady flow configurations efficiently, with reduced computational cost and stable solution quality, in order to allow meaningful comparison with other methods. Therefore, based on figures 18 and 19, the decision to simply omit particles near the hub for the first three rotations proved to be a reasonable trade-off between numerical stability and computational cost.

This configuration was then selected, and new simulations were run at various operating points. The results obtained with the VPM method (NS-based Lagrangian method via FLOWUnsteady) were compared against those from BEMT (analytical approach using XFOIL polars) and extrapolated experimental data provided by Vertical Aerospace, as shown in Figure 19.

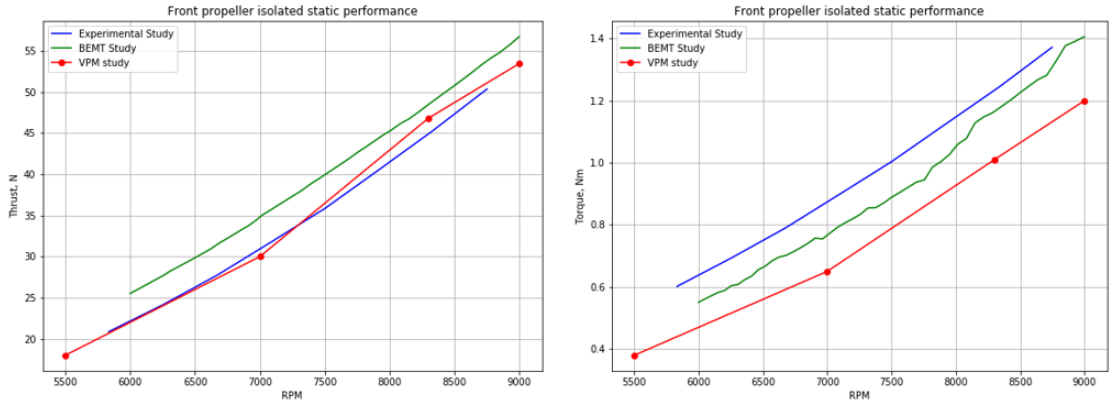

Figure 20: Results of the front propeller isolated static performance of the experimental, BEMT and VPM methods

In Figure 20, all three methods exhibit similar overall trends. However, one would expect the VPM and BEMT results to align more closely, as both approaches use the same XFOIL airfoil polars to model the blades. While the simulation setup provided stable and converged results within a reasonable computation time, the performance of the VPM method still appeared somewhat disappointing when compared to the BEMT predictions.

4.2.2. Aft rotor

For the aft rotor, the same setup as defined for the front rotor was used. The VPM results could only be compared to the approximate experimental data provided by Vertical Aerospace, as shown in Figure 21.

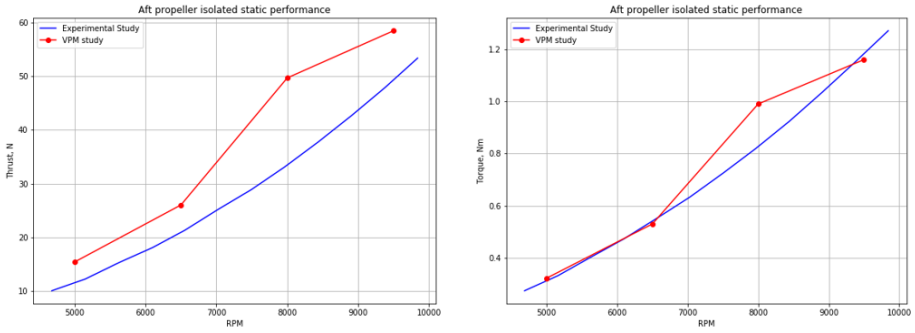

Figure 21: Results of the aft propeller static performance of the Experimental and VPM methods

The results from the VPM method and the experimental data showed similar trends, although at 8000 RPM there appeared to be an overestimation in the VPM results.

4.3. Transition Climb and Transition Descent

As the project progressed and based on the knowledge gained from the previous investigations, the transition climb and transition descent cases became particularly interesting to study from an aerodynamic perspective. These cases combine the different flow conditions observed in the cruise and hover cases. Indeed, in these configurations, both the front and rear rotors were simulated simultaneously, allowing the aerodynamic interactions between the two rotors to be observed and highlighted.

4.3.1. Transition Climb

- **Definition of the parameters**

The transition climb is a particular flight condition that occurs during the transition phase of an eVTOL aircraft from vertical to horizontal flight. In this regime, both propellers experience a combination of horizontal and vertical inflow velocities, and the front propeller is tilted forward relative to the aircraft axis. In the studied case: horizontal velocity $V_{horizontal} = 24.9\, m/s$, vertical velocity $V_{vertical} = 2.18\, m/s$, tilt angle of the propeller $50°$. In FLOWUnsteady, three key parameters were used to define the inflow and propeller orientation in space for such a case: *MagVinf* the magnitude of the inflow velocity vector, the *AoA* (Angle of Attack) the inclination angle of the inflow vector in the global reference frame (here, the xz-plane) and the *propeller orientation* defined independently of the inflow direction and given by the propeller tilt in 3D space, see figure 22.

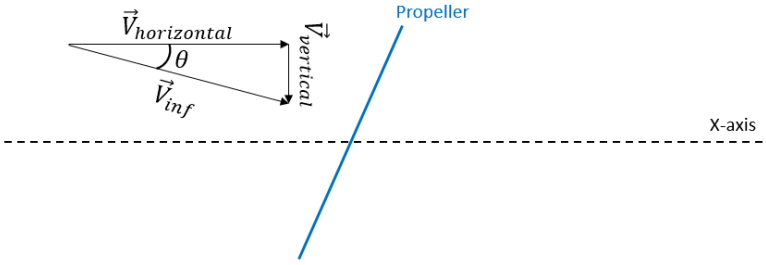

Figure 22: Definition of the different velocities in the front of the propeller in the transition climb configuration

To compute the input parameters:

$$V_{inf} = \sqrt{{V_{horizontal}}^2 + {V_{vertical}}^2} = \sqrt{24.9^2 + 2.18^2} = 25\ m/s \quad \textbf{(9)}$$

$$\theta = \arctan\left(\frac{V_{vertical}}{V_{horizontal}}\right) = \arctan\left(\frac{2.18}{24.9}\right) \approx 5° \quad \textbf{(10)}$$

The 55° total tilt angle corresponds to the orientation of the front propeller, not the inflow. The inflow itself only has an AoA of 5°, computed from the velocity vector. This distinction is critical when setting up simulations, especially in vortex methods where freestream orientation and body orientation are defined separately.

- **Aerodynamic analysis**

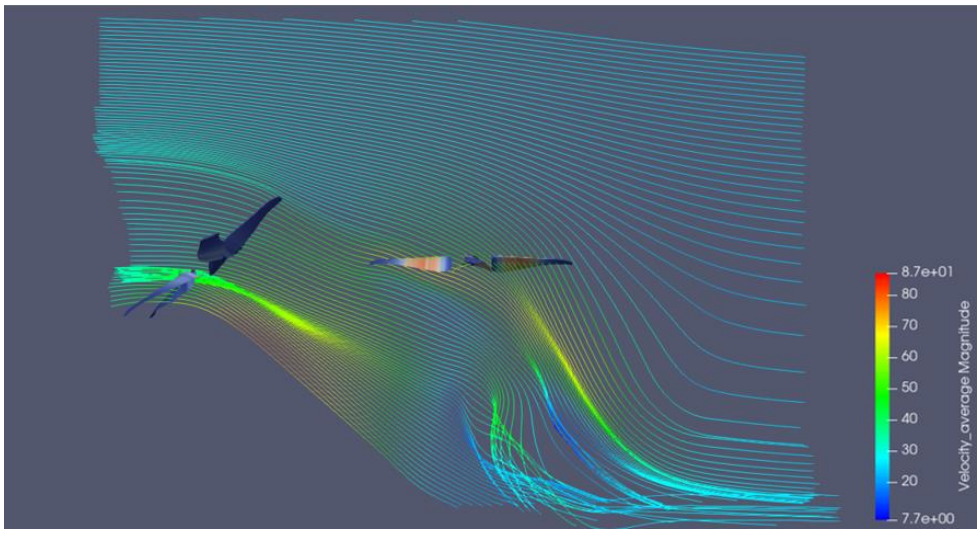

Figure 23: Longitudinal view of the aerodynamic behaviour in the transition climb configuration, illustrating the variation of the axial velocity within Paraview over one rotation; streamlines are shown

Figure 23 depicts the flow around two axially aligned rotors, with the upstream rotor (left) producing a well-defined wake characterized by accelerated, curved streamlines and a high-velocity jet (60–70 m/s) deflected downward and laterally (–z, +y). The downstream rotor lies directly in the path of this disturbed flow, resulting in significant aerodynamic interaction. The inflow is highly non-uniform, with faster velocities on the left side and slower ones on the right, causing streamline asymmetry and potential aerodynamic imbalance across the rotor disk. Its own wake, influenced by upstream disturbances, shows reduced velocities and lateral deflection to the left. A stagnation or recirculation zone near the root (dark blue) suggests low-pressure or reversed flow, pointing to unsteady behaviour.
Overall, the strong aerodynamic coupling between rotors causes flow concentration at the mid-plane and potential unsteady interactions. These effects, non-uniform inflow, reduced thrust, pressure fluctuations, and asymmetry, highlight the need for optimized rotor layout (axial spacing, offset, or phasing) to improve system stability and efficiency.

4.3.2. Transition descent

- **Definition of the parameter**

In this regime, both propellers experience a combination of horizontal and vertical inflow velocities, and the front propeller is tilted forward relative to the aircraft axis. In the studied case: horizontal velocity $V_{horizontal} = 24.9\, m/s$, vertical velocity $V_{vertical} = -2.18\, m/s$, tilt angle of the propeller $100°$.

As described previously in the transition climb, three key parameters were used to define the inflow and propeller orientation in space for such a case: *MagVinf* the magnitude of the inflow velocity vector, the *AoA* (Angle of Attack) the inclination angle of the inflow vector in the global reference frame (here, the xz-plane) and the *propeller orientation* defined independently of the inflow direction and given by the propeller tilt in 3D space, see figure 24.

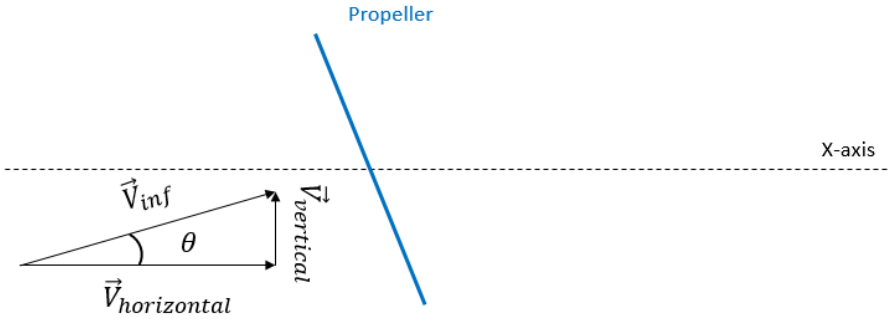

Figure 24: Definition of the different velocities in the front of the propeller in the transition descent configuration

To compute the input parameters:

$$V_{inf} = \sqrt{{V_{horizontal}}^2 + {V_{vertical}}^2} = \sqrt{24.9^2 + (-2.18)^2} = 25\, m/s \quad \textbf{(11)}$$

$$\theta = \arctan\left(\frac{V_{vertical}}{V_{horizontal}}\right) = \arctan\left(\frac{-2.18}{24.9}\right) \approx -5° \quad \textbf{(12)}$$

The 105° total tilt angle corresponds to the orientation of the front propeller, not the inflow. The inflow itself only has an AoA of -5°, computed from the velocity vector. This distinction is critical when setting up simulations, especially in vortex methods where freestream orientation and body orientation are defined separately.

- **Aerodynamic analysis**

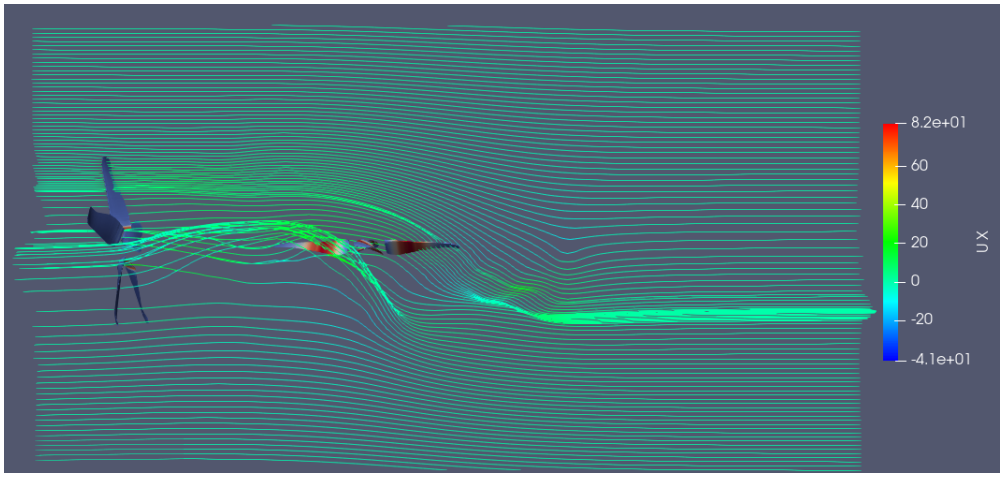

Figure 25: Profile view of the aerodynamic behaviour in the transition descent configuration, illustrating the variation of the axial velocity within Paraview

Figure 25 shows a side view (x–z plane) of the flow past two rotors in a transition descent configuration: the front rotor (left) is tilted backward at 110°, while the rear rotor (right) remains nearly horizontal. The inclined front rotor generates a strong downward-rearward jet (green to red streamlines), leading to significant flow distortion and asymmetry for the rear rotor.

Part of the front rotor's wake recirculates into the domain (blue areas with negative U_x), suggesting wake re-ingestion and unsteady blade loading. Its wake impacts the lower portion of the rear rotor, while the upper part experiences slow or reversed flow, creating uneven aerodynamic conditions.

This asymmetry likely causes performance degradation, with the rear rotor experiencing partial stall or reversed flow near the top and high-speed inflow near the bottom. Its wake appears unstructured and deflected, indicating reduced efficiency and increased unsteadiness.

Two key features stand out: a recirculation zone above the rotor plane due to the tilt of the front rotor, and a jet impingement zone at the base of the second rotor. These contribute to strong three-dimensional flow, pressure fluctuations, and transient aerodynamic loads.

Overall, the tilted rotor induces complex flow interactions, non-uniform inflow, thrust imbalance, potential stall, and increased noise or vibration, underlining the importance of rotor tilt and placement in transition flight phases.

5. Observations

This final internship marks the end of my engineering studies and completes almost a full year at the Institute of Propulsion Technology – Engine Acoustics Department at the German Aerospace Center (DLR) in Berlin. Over this period, I significantly strengthened my skills in numerical simulation and CFD, particularly in the context of aerodynamics and propeller analysis. Although most tools and methods were new to me, I adapted quickly, and the strong support from my supervisors allowed me to learn efficiently and deepen my understanding.

The internship was structured around a long-term project, which offered the opportunity to explore more concrete and applied aspects of simulation work. It was a natural continuation of my previous Sigma+ internship at DLR, and helped me grow in both technical ability and professional maturity. One major challenge I faced was solving a numerical issue in one configuration, which required time, patience, and a methodical approach.

On a professional level, the regular daily and weekly meetings were a real asset, allowing for ongoing feedback, clear objectives, and in-depth discussions about the physical interpretation of the results. This collaborative environment made the experience both motivating and intellectually enriching.

From a personal and intercultural standpoint, working at DLR was highly rewarding. I discovered a research culture focused on rigor and collaboration, within a team that was both passionate and welcoming. The demanding but supportive environment helped me develop autonomy, resilience, and confirmed my interest in pursuing a career in aerodynamics.

6. Conclusion and outlook

6.1. Conclusion

During the internship, knowledge gained during the first research placement was applied to the ENODISE model. The Vortex Particle Method (VPM) was successfully validated on the ENODISE B1 configuration, highlighting aerodynamic interaction phenomena between the rotors that can contribute to noise generation—thus establishing a clear link between aerodynamics and acoustics.

This expertise was subsequently transferred to the rotor geometries of the eVTOLUTION project, covering various flight configurations to validate the method on a new, more complex setup. The results showed that the method performs well in configurations involving predominantly axial flow, such as cruise, transition climb, and transition descent. However, the hover case, particularly without initial induced velocity, remains numerically more challenging and requires further refinement.

Although the VPM method delivered consistent results for the cruise condition, the comparison with BEMT predictions raised some open questions, as closer agreement was initially expected given the use of the same airfoil data. These differences underline the need for a deeper understanding of the modeling assumptions and flow behavior in both approaches before drawing firm conclusions.

6.2. Outlook

The work presented has shown important progress in applying the VPM method for flow simulations on rotor models. Nonetheless, several challenges remain to fully validate this approach, particularly for the eVTOLUTION models, before extending it confidently to other propeller configurations.

Specifically, the hover case revealed numerical difficulties due to the lack of initial induced velocity, highlighting the need for improved treatment of low-flow or stagnation regions. Furthermore, while the VPM method performed well in cruise and transition flight conditions, the comparison with the BEMT method showed discrepancies that require further investigation to understand the sources of these differences despite using the same aerodynamic polars for the airfoils.

Future work should focus on refining the numerical stability and accuracy of the method in challenging flow conditions, especially hover. Additionally, expanding the validation to include more complex geometries and flight scenarios, such as dynamic rotor tilting or the presence of downstream aerodynamic surfaces, would provide a more comprehensive assessment.

Finally, since the aerodynamic phenomena are closely linked to acoustic emissions, integrating aeroacoustics simulations will be essential to fully understand and predict noise generation mechanisms. Extending the study to couple aerodynamic and acoustic analyses will thus be a crucial next step, especially for applications in eVTOL aircraft design.

7. Bibliography

[1]: Institute of Technology Propulsion (dlr.de)

[2]: D. Ferretto (POLITO), N. Viola (POLITO), S. Guérin (DLR), S. Srivastava (GKN), N. Dhiman (TUD), Y. Chance (TUD), C. Mead (VAERO), *eVTOL mUlti-fideliTy hybrid design and Optimization for low Noise and high aerodynamic performance*, WP3 technical report

[3]: https://flow.byu.edu/FLOWUnsteady/

[4]: E. J. Alvarez & A. Ning (2022), *"Meshless Large Eddy Simulation of Rotor-Wing Interactions Through the Reformulated Vortex Particle Method,"*

[5]: Tobias Lade, Master Thesis, *“Method development for predicting propeller noise for border shift intake in the low Reynolds number area,”*

[6]: https://evtolution.eu/

[7] : J. Gordon Leishman, Aerodynamics of Airfoil Sections – Introduction to Aerospace Flight Vehicles

Appendix A

Model	Description
A1	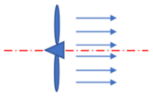 single rotor
A2	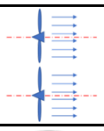 tandem side-by-side rotors, co and contra-rotating
A4	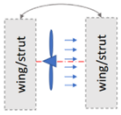 single rotor upstream/downstream of strut or simplified airfoil shape
B1	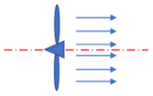 single rotor with flight effects, with its rotation axis at different angles with respect to the incoming flow, with or without incoming grid-generated turbulence figuring the ingestion of atmospheric turbulence
B2	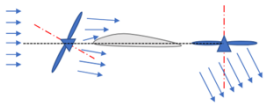 tandem rotor + airframes in presence of flight effects, with the front rotor at various tilt angles with respect to the incoming flow

Appendix B

		Hover	Transition climb	Cruise	Transition descent	Emergency point (only aerodynamic)
Flight condition	Thrust	A/C weight+10%		6.8 N		
	Uhorizontal	0 m/s	24.9	61 m/s	24.9	0
	Uvertical	0 m/s	2.18	0 m/s	-2.18	0
	Pamb	101325 Pa	101325	101325	101325	101325
	Tamb	25°C	25°C	25°C	25°C	25°C
Front rotor (nominal value)	RPM (downscaled)	8300	11500	8000	7500	12000
	AoA wrt. aircraft axis	90°	50° tilt + 5° AoA = 55°	0°	100° tilt + 5° AoA = 105°	90°
	Blade pitch angle	Hover pitch (as provided)	Hover pitch	Cruise pitch (hover − 14°)	Hover pitch	Hover pitch
Benchmark for front rotor	RPM (downscaled)	8300	11500	8000 rpm for 30 m/s	7500	
	AoA wrt. aircraft axis	90°	50° tilt + 5° AoA = 55°	0°	100° tilt + 5° AoA = 105°	
	Blade pitch angle	Hover pitch	Hover pitch	(Current+14°)	Hover pitch	
Aft rotor (nominal value)	RPM (downscaled)	8900	9100		9300	12000
	AoA wrt. aircraft axis	90°	90°		90°	90°
	Blade pitch angle	Hover pitch	Hover pitch		Hover pitch	Hover pitch
Benchmark for aft rotor	RPM (downscaled)	8900	9100		9300	
	AoA wrt. aircraft axis	90°	90°		90°	
	Blade pitch angle	Hover pitch	Hover pitch		Hover pitch	

Appendix C

- **Cruise (left) and Hover (right):**

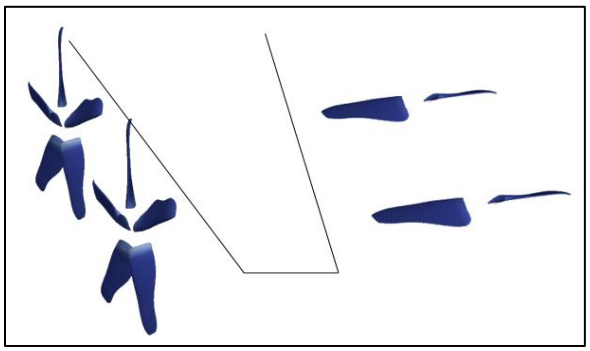

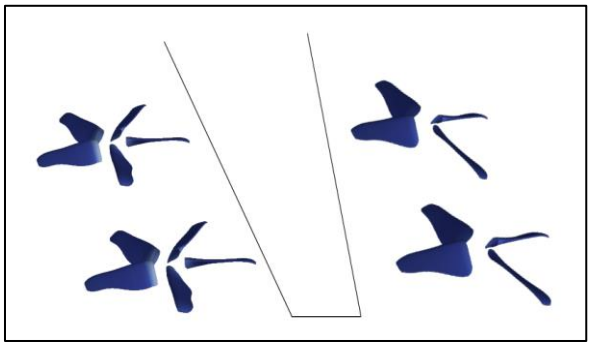

- **Transition Climb (left) and Transition Descent (right):**